

## SIMULATION OF TURING PATTERNS IN A CHEMICAL REACTION-DIFFUSION SYSTEM

ERIK MOSEKILDE and OLE JENSEN

Physics Department, The Technical University of Denmark,  
2800 Lyngby, Denmark

GUY DEWEL and PIERRE BORCKMANS

Service de Chimie Physique, Université Libre de Bruxelles,  
B-1050 Brussels, Belgium

**Abstract** The emergence, growth and stabilization of stationary concentration patterns in a chemical reaction-diffusion system are studied by numerical simulations of the Lengyel-Epstein model. This model represents a key to understanding the recently obtained Turing structures in the chlorite-iodide-malonic acid system.

### INTRODUCTION

One of the most fundamental problems in theoretical biology is to explain the mechanisms by which patterns and forms are created in the living world. In his seminal paper on *The Chemical Basis of Morphogenesis*, Turing<sup>1</sup> showed how chemical reaction-diffusion systems under certain conditions could become unstable and yield to the growth of stationary concentration

patterns. Turing also suggested that the emergence of such patterns could play a major role in biological form formation.

In its simplest form, the Turing instability arises from the interaction of two chemical species: an activator and an inhibitor. The activator is autocatalytic so that the rate at which this species is produced increases with its concentration. More activator also augments the inhibitor production. This species, on the other hand, reduces the rate of production for the activator. A general condition for the instability to occur is that the inhibitor diffuses significantly faster than the activator. If, under this condition, a random fluctuation of the chemical concentrations has produced a local surplus of activator, the concentration of this species will start to build up. The activator also produces more inhibitor, but this species diffuses more rapidly and spreads into the surrounding area. Here it suppresses the activation process while in the original region the dilution of the inhibitor concentration allows the activator concentration to continue to grow, until it is finally limited by nonlinear constraints.

Over the years Turing's ideas have attracted the attention of a great number of investigators. A variety of different model systems have been proposed<sup>2,3</sup>, the basic theoretical aspects of the problem have been studied in considerable detail<sup>4-8</sup>, and it has been illustrated in principle how biological patterns can arise from the Turing instability<sup>9</sup>.

Working with the chlorite-iodide-malonic acid or so-called CIMA reaction, which under other circumstances is known to produce oscillations, bistability and traveling waves, De Kepper and his coworkers<sup>10</sup> discovered the formation of stationary three-dimensional structures with characteristic wavelengths of 0.2 mm. The structures were confined to the center of the reactor by the feeding gradients. By using an inert gel as the reaction

medium, a continuous supply of fresh reactants could be maintained while at the same time avoiding convection. To allow visualization starch was used as a color indicator. Starch forms a reversible complex with iodine which is practically immobile in the gel. The effect is a reduction of the diffusion rate for the activator (iodide), providing the required difference in the diffusion constants.

Subsequent studies by Ouyang and Swinney<sup>11</sup> using a disk reactor showed quasi two-dimensional patterns in the form of hexagons and stripes and also lead to an experimental determination of the bifurcation diagram for the Turing instability. By means of light absorption techniques, Lengyel et al.<sup>12</sup> were able to establish the form of the rate laws for the most essential processes in the CIMA reaction. After proper renormalization and including the diffusion terms they proposed the following two-variable model:

$$\frac{\partial u}{\partial t} = a - u - \frac{4uv}{1+u^2} + \nabla^2 u \quad (1)$$

and

$$\frac{\partial v}{\partial t} = \delta \left[ b \left( u - \frac{uv}{1+u^2} \right) + c \nabla^2 v \right] \quad (2)$$

Here,  $u$  represents the concentration of iodide ions (activator) and  $v$  the concentration of chlorite ions (inhibitor).  $a$  and  $b$  are parameters that are related to the feed concentrations. A shift towards higher values of  $a$  represents an increase in the supply of malonic acid relative to the supply of chlorine dioxide. Likewise, increasing  $b$  corresponds to a higher supply of iodine.  $c$  is the ratio of the diffusion constant for chlorite to that of uncomplexed iodide, and  $\delta$  is a rescaling parameter which primarily depends on the concentration of starch. The higher this concentration is, the larger  $\delta$  will be. The effective ratio of the diffusion constants hereafter becomes  $\delta c$ . In the simulations to be presented below we have taken  $c = 1.5$  and  $\delta = 8$ .  $a$

and  $b$  are used as control parameters. Simulations with the Lengyel-Epstein model have previously been published by Jensen *et al.*<sup>13, 14</sup>

## SIMULATION RESULTS

The Lengyel-Epstein model exhibits a unique homogeneous steady state  $(u_0, v_0) = (a/5, 1 + a^2/25)$ . If diffusion is neglected ( $\nabla^2 u = \nabla^2 v = 0$ ), the homogeneous steady state is stable for  $b > b_H = (-5^3 + 3a^2)/5a\delta$  where a Hopf bifurcation producing self-sustained oscillations occurs<sup>12</sup>. A nonlinear analysis shows that the Hopf bifurcation is slightly inverted (or subcritical) for  $a > 17.5$ . Hence, hysteresis occurs, and the stable limit cycle is generated with a finite amplitude. When diffusion is taken into account, the linear stability analysis shows that the system becomes unstable towards stationary spatial perturbations of finite wave number for

$$b < b_T = \frac{(5^3 + 13a^2 - 4a\sqrt{10(5^2 + a^2)})c}{5a} \quad (3)$$

The wave number  $k_c$  at which the Turing instability first occurs is given by

$$k_c^2 = \sqrt{\frac{25ab}{(25 + a^2)c}} \quad (4)$$

We note that the Turing threshold  $b_T$  is independent of  $\delta$ . On the other hand, the Hopf bifurcation point  $b_H$  varies inversely with  $\delta$ . Hence, for sufficiently high concentrations of starch,  $b_T > b_H$ , and a region exists in which the homogeneous steady state is stable towards uniform oscillations, but unstable with respect to the development of spatial concentration patterns.

Figure 1 shows the growth of a one-dimensional Turing structure out of the homogeneous steady state for  $a = 30$  and  $b = 2.8$ . The numerical calculations were performed by means of a semi-implicit Crank-Nicolson method with no-flux boundary conditions. The calculations were seeded

with low intensity noise to represent slight inhomogeneities and thermal fluctuations in the concentrations of the chemical species. The incubation time for the structure to emerge is determined by the rate of growth of the most unstable modes and the range over which they have to be amplified to reach macroscopic significance. At low aspect ratios (i.e. for systems which only span a few wavelengths), the boundary conditions influence the mode selection. However, this influence disappears for larger systems.

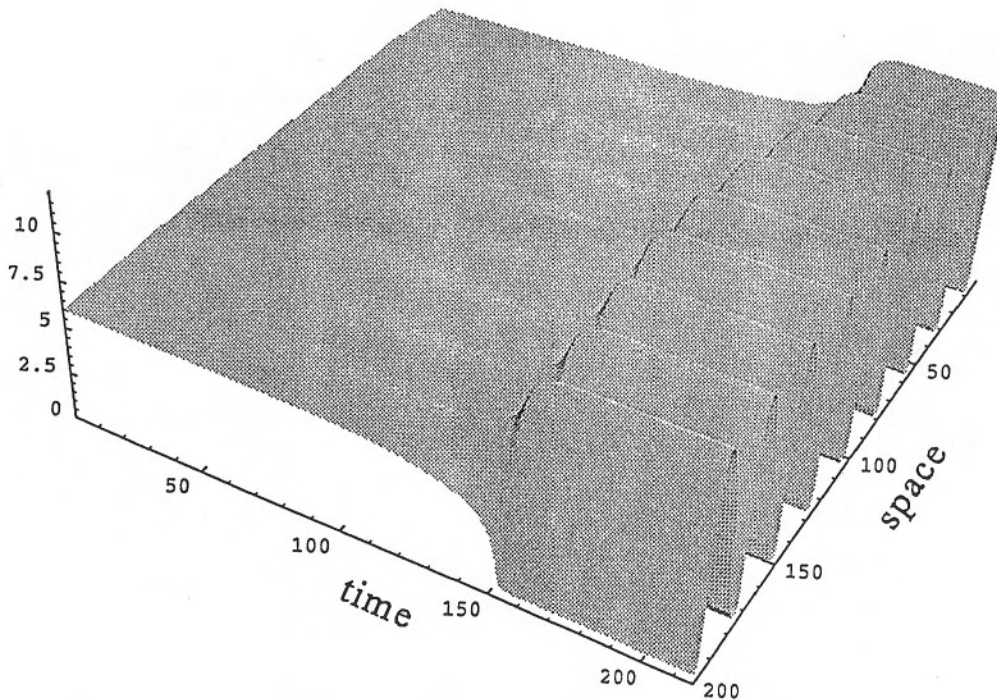


FIGURE 1. Growth of a one-dimensional Turing structure out of the homogeneous steady state.

Figure 2 shows the bifurcation diagram for the Lengyel-Epstein model with one spatial dimension. Starting with  $b$  in the interval for Turing instabilities ( $b_H < b < b_T$ ), the diagram was obtained by seeding the homogeneous steady state with noise to obtain the stationary pattern and determine its

amplitude. Hereafter this pattern was used as initial conditions when restarting the integration with a slightly different value of  $b$ . With this *adiabatic* approach we could follow the amplitude of the stationary structure as a function of  $b$  into the region  $b > b_H$  where it can only grow out of the homogeneous steady state by applying finite amplitude perturbations. In each simulation the stability of the structure was tested by applying a small noise signal. A similar approach was used to obtain the bifurcation curve for the Hopf oscillations.

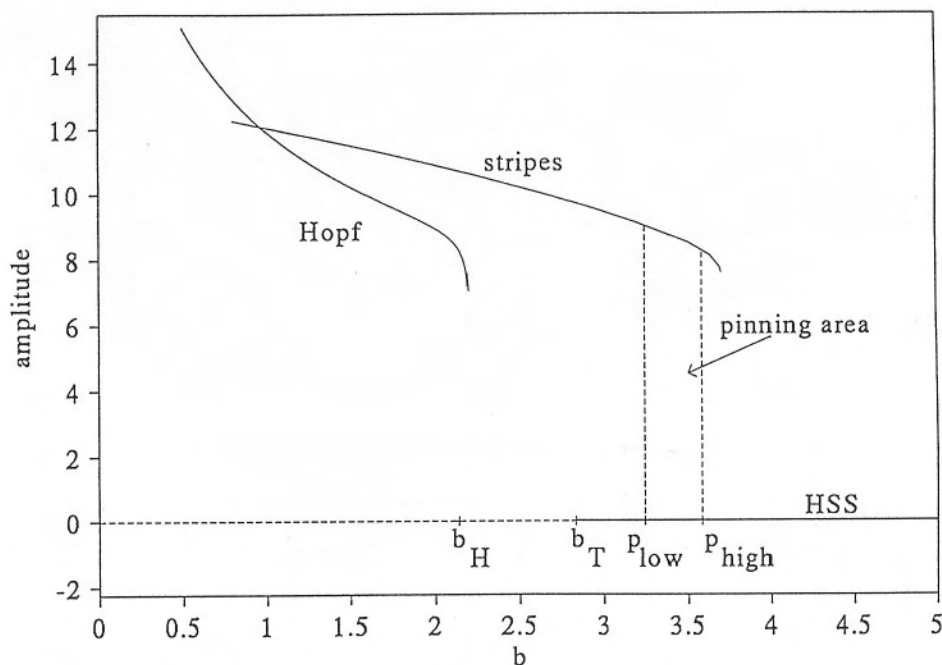


FIGURE 2. Numerically obtained bifurcation diagram for the one-dimensional Lengyel-Epstein model with  $\alpha = 30$ .

For  $b > p_{high}$ , the homogeneous steady state dominates, and a front separating this state from a region with Turing stripes will propagate into the

Turing area. For  $b < p_{low}$  the opposite occurs. However, in the region  $p_{low} < b < p_{high}$ , the front is unable to propagate, and stable localized structures may exist. For instance, we may have a region with Turing stripes surrounded by a sea of homogeneous steady state<sup>13</sup>. For  $b < 2.1$ , the stability domains for Turing structures and uniform temporal oscillations overlap. Here, we may have a front between a region with Turing stripes and a region with Hopf oscillations. In an interval around  $b = 1.5$ , this front appears to be stationary. For lower values of  $b$ , the Hopf oscillations will invade the Turing area and vice versa for larger values of  $b$ . For  $b < 1.0$  one typically observes that a stripe structure grows up from the noise inflicted homogeneous steady state and reaches a certain amplitude, before the entire system switches to a mode of uniform temporal oscillations.

In two dimensions the picture is even more complicated. Here, we have the possibilities of hexagons or stripes, and both types of structure have been experimentally observed<sup>11</sup>. Moreover, for hexagons the phase is important, since the activator can show either concentration maxima or minima in the centers of the hexagons. Figure 3 shows a three-dimensional representation of the concentration profile for a hexagonal structure. As in figure 1, the pattern has grown from the homogeneous steady state perturbed by low amplitude noise. It clearly reveals a number of defects arising from the fact that at different locations patterns start to form with different orientations. Once formed, the patterns may adjust a little. However, the original misalignment is never completely removed. The hexagonal patterns tend to become more regular as  $b$  is increased from 2.5 (as in figure 3) towards the Turing bifurcation point at  $b \cong 2.8$ . If  $b$  is reduced, on the other hand, even more irregular patterns emerge.

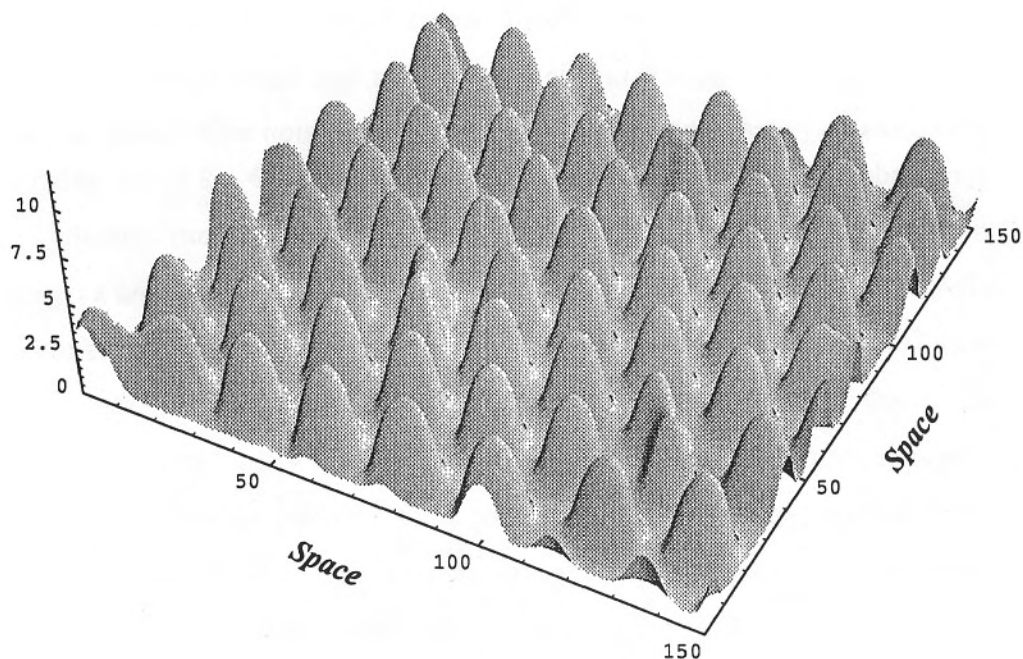


FIGURE 3. Concentration profile for a typical hexagonal structure.  $\alpha = 30$  and  $b = 2.5$ .

For comparison with the experimental results obtained with the strip reactor, we have also tried to simulate the structures which arise when a gradient in feed concentration is applied to the system. The results of such a simulation in which  $b$  varies linearly from 1.2 to 2 over the investigated spatial domain are shown on figure 4. Here  $\alpha = 20$ . In the forefront of the figure we observe a region of homogeneous steady state. Hereafter a band with stripes follows, again followed by a transition to hexagons in the far end of the figure. In other cases we have found that hexagons arise between the region with homogeneous steady state and the region with stripes. In the actual experiment the concentration gradient may not be constant as in our simulation.



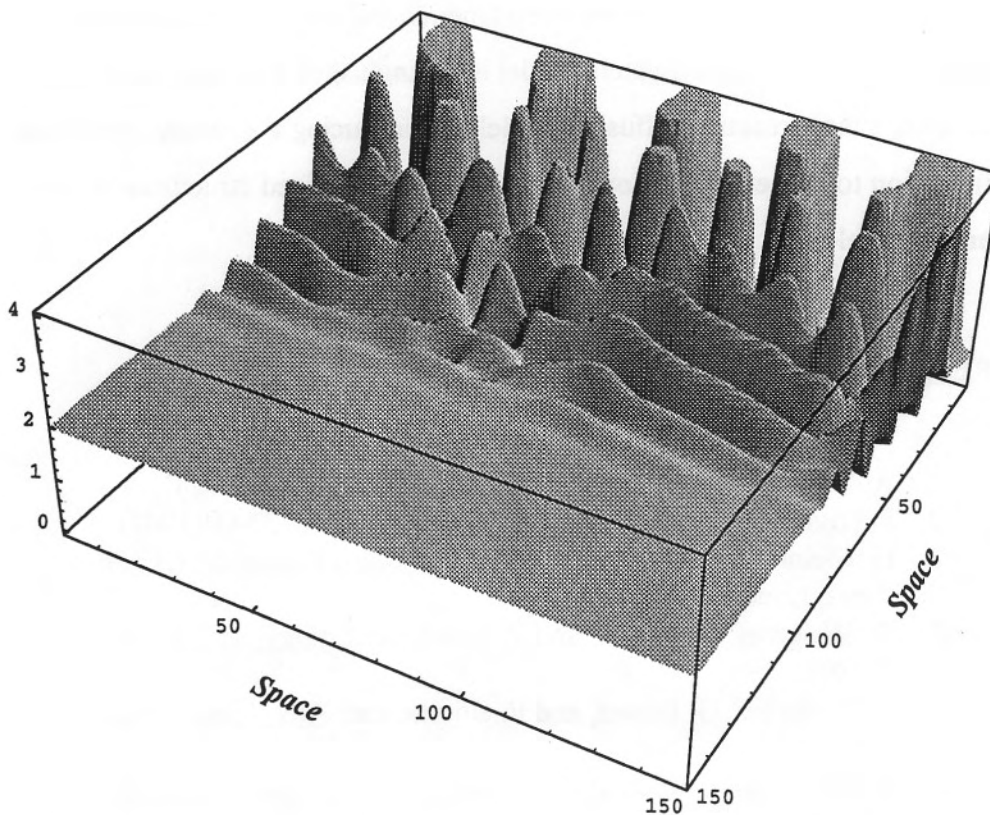


FIGURE 4. Transitions from homogeneous steady state to stripes to hexagons when a gradient in  $b$  is applied to the system.  $a = 20$ .

## CONCLUSION

The observation of Turing structures under laboratory conditions represents a significant breakthrough for one of the most fundamental ideas in morphogenesis and biological pattern formation. This success, which had to await the development of new types of gel reactors, is based on a combination of an oscillatory chemical reaction with a process that rescales the diffusion constant of the activator species. This discovery has naturally prompted a rapidly growing interest into the search for new types of structures. In parallel with this there is a need to extend the theoretical

analysis to study the relation between kinetics and the types of patterns produced. The Lengyel-Epstein model is distinguished from previously studied, simple reaction diffusion models by producing a strongly subcritical transition to stripes. This allows for a variety of localized structures to exist and be stable<sup>13,14</sup>.

## REFERENCES

1. A. Turing, Phil. Trans. R. Soc. Lond. B, **237**, 37 (1952)
2. I. Prigogine and G. Nicolis, J. Chem. Phys., **46**, 3543 (1967)
3. H. Meinhardt, Models of Biological Pattern Formation (Academic Press, London, 1982)
4. D. Walgraef, G. Dewel, and P. Borckmans, Phys. Rev. A, **21**, 397 (1980)
5. D. Walgraef, G. Dewel, and P. Borckmans, Adv. Chem. Phys., **49**, 311 (1982)
6. P. Borckmans, A. De Wit, and G. Dewel, Physica A, **188**, 137 (1992)
7. A. De Wit, G. Dewel, P. Borckmans, and D. Walgraef, Physica D, **61**, 289 (1992)
8. J. Verdasca, A. De Wit, G. Dewel, and P. Borckmans, Phys. Lett. A, **168**, 194 (1992)
9. J.D. Murray, Mathematical Biology (Springer, Heidelberg, 1989)
10. V. Castets, E. Dulos, J. Boissonade, and P. De Kepper, Phys. Rev. Lett., **64**, 2953 (1990)
11. Q. Ouyang and H.L. Swinney, Nature (London) **352**, 610 (1991)
12. I. Lengyel and I.R. Epstein, Proc. Natl. Acad. Sci. USA, **89**, 3977 (1992)
13. O. Jensen, V.O. Pannbacker, G. Dewel, and P. Borckmans, Phys. Lett. A, **179**, 91 (1993)
14. O. Jensen, V.O. Pannbacker, E. Mosekilde, G. Dewel, and P. Borckmans, Phys. Rev. E, **50**, 736 (1994)